Chinese Journal of Polymer Science Vol. 34, No. 9, (2016), 1158–1171

Chinese Journal of Polymer Science

Effect of Long Chain Branching on the Rheological Behavior, Crystallization and Mechanical Properties of Polypropylene Random Copolymer*

Jing Cao, Na Wen and Yu-ying Zheng**
College of Materials Science and Engineering, Fuzhou University, Fuzhou 350108, China

Abstract Long chain branched polypropylene random copolymers (LCB-PPRs) were prepared *via* reactive extrusion with the addition of dicumyl peroxide (DCP) and various amounts of 1,6-hexanediol diacrylate (HDDA) into PPR. Fourier transform infrared spectrometer (FTIR) was applied to confirm the existence of branching and investigate the grafting degree for the modified PPRs. Melt flow index (MFI) and oscillatory shear rheological properties including complex viscosity, storage modulus, loss tangent and the Cole-Cole plots were studied to differentiate the LCB-PPRs from linear PPR. Differential scanning calorimetry (DSC) and polarized light microscopy (PLM) were used to study the melting and crystallization behavior and the spherulite morphology, respectively. Qualitative and quantitative analyses of rheological curves demonstrated the existence of LCB. The effect of the LCB on crystalline morphology, crystallization behavior and molecular mobility, and, thereby, the mechanical properties were studied and analyzed. Due to the entanglements between molecular chains and the nucleating effect of LCB, LCB-PPRs showed higher crystallization temperature and crystallinity, higher crystallization rate, more uniformly dispersed and much smaller crystallite compared with virgin PPR, thus giving rise to significantly improve impact strength. Moreover, the LCB-PPRs exhibited the improved yield strength. The mobility of the molecular chain segments, as demonstrated by dynamic mechanical analysis (DMA), was improved for the modified PPRs, which also contributed to the improvement of their mechanical properties.

Keywords: Polypropylene random copolymer; Long chain branch; Rheological properties; Mechanical properties.

INTRODUCTION

Polypropylene random copolymer (PPR), with the random insertion of 1 wt%–7 wt% of ethylene along the polypropylene chains, is one kind of commercial polypropylene (PP), a semicrystalline polymer with a number of desirable properties. PPR plays an important role in film, rigid packaging and pipe applications due to its desirable balance of clarity, flexibility and mechanical strength with respect to polypropylene homopolymer (PPH)[1, 2]. The fact is because the random insertion of ethylene along the PPH chains promotes the formation of shorter stereoregular blocks and decreases the melting temperature and crystallinity[3]. However, commercial PPR produced with Ziegler-Natta or metallocene catalysts results in high linear chains and a relatively narrow molecular weight distribution. Similar with linear PPH, linear PPR has relatively low melt strength. Wang *et al*.[4] has demonstrated that entangled linear polymers cannot attain steady flow during startup uniaxial extension. That is to say, the melts of linear chain systems and their blends fail after yielding over a wide range of rates in the form of non-uniform extension without ever reaching a fully developed flow state. Therefore, the

* This work was financially supported by the Foundation for Development of Science and Technology of Fuzhou University (No. 2011-XY-1).
** Corresponding author: Yu-ying Zheng (郑玉婴), E-mail: yyzheng@fzu.edu.cn
Received February 6, 2016; Revised March 18, 2016; Accepted May 5, 2016
doi:10.1007/s10118-016-1830-4

rheological behavior of linear PPR is not fitting for the processes where elongational flows are dominant, such as blowing, thermoforming, or foaming. Thus it's important to improve its above properties. The researches on high melt strength PP have drawn more and more attentions recently[5–9].

"High melt strength PP'' can be produced by introducing long chain branching (LCB) into linear PP[10, 11]. LCB structure can improve the processability of PP, including strain hardening and shear thinning under melt conditions, thus could broaden the applications of PP. There are several methods to prepare branching PP. Some works reported on the direct synthesis of LCB-PPR using metallocene catalysis[12–14]. However, this method is only used in the laboratory. Generally, two techniques have been developed to prepare LCB polypropylene (LCB-PP) in industry: electron beam irradiation[15, 16] and reactive extrusion processes[17–21]. Compared to electron beam irradiation, the reactive extrusion has many advantages, such as simple operation, low cost, and high productivity. As a result, the preparation of LCB-PP by reactive extrusion has been used more and more over the past few decades.

For the reactive extrusion process, peroxide free-radical initiator and a polyfunctional monomer were usually introduced simultaneously into polypropylene to form graft structure on the backbone of PP. The characteristics of polymers with LCBs on a molecular level can be identified by a comparative measurement of polymer hydrodynamic volume in a dilute solution, with the help of GPC coupled with on-line light scattering (LS), viscosity (CV)[22, 23] and/or differential reflective index (DRI) detectors[24, 25].

More recently, ^{13}C-NMR measurements detected branching levels of 0.35 branches per 10000 carbons in polyethylenes[26]. Since the flow behavior of polymers is sensitive to long chain branches at concentrations far below the detection limit of the above methods, rheology becomes another feasible way to identify low levels of this type of branching[27].

The present researches basically focus on the rheological properties and chemical structure of LCB PP, while the crystallization behavior, morphology and the mechanical properties of the modified PP, which are very important in the practical applications, have only been reported by few authors[28]. Moreover, some researchers have only investigated LCB PP with a certain amount of LCB, while the characterization of the structure, crystallization behavior and mechanical properties of LCB PP with various contents of LCB have not been studied. In addition, the mobility of the molecular chains has not been studied. Furthermore, the previous research has generally been based on the modification of PPH, while very few researches are based on the modification of PP copolymers[3]. Therefore, in this paper, PPR was modified in the presence of a certain amount of peroxide and various amounts of polyfunctional monomer by reactive extrusion to obtain PPRs with various contents of LCB; comprehensive characteristics, including the melt flow index, rheological properties, crystallization behavior and morphology, mechanical properties as well as the mobility of molecular chain segments with different contents of LCB are studied. Effect of LCB on the rheological behavior, crystalline morphology, crystallization behavior and molecular mobility, and thereby the mechanical properties are studied and analyzed in detail.

EXPERIMENTAL

Materials

The material was a PPR with a melt flow rate of 2.2 g/10min (230 °C/2.16kg) and a density of 0.900 g/cm^3, supplied by LyondellBasell Industries (Netherlands). The PPR pellets were stabilized by the addition of 0.1% antioxidant Irganox 1010 (Jinhai Albemarle; China). Dicumyl peroxide (DCP) was purchased from China National Medicine Group (Shanghai Reagent Corp., China). 1,6-Hexanediol diacrylate (HDDA) was obtained from Beijing Eastern Acrylic Chemical Technology Co., Ltd. (China). The chemical structure of HDDA is displayed in Fig. 1.

Sample Preparation

To achieve homogenous dispersion of the additives in the PPR pellets, DCP and HDDA were dissolved in 50 mL of acetone, and then the solution was added to 800 g of PPR pellets and mixed for 10 min in a high-speed mixer.

After mixing, the modification was carried out in a corotating twin-screw extruder. The temperatures of the extruder zones were maintained at 170, 180, 190, 190, 200, and 205 °C from hopper to die. The constituents of virgin and modified PPRs with DCP and various concentrations of HDDA are listed in Table 1.

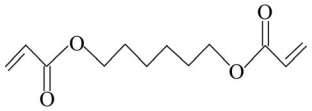

Fig. 1 The chemical structure of HDDA

Table 1. Constituents of virgin and modified PPRs

Samples	PPR (g)	DCP (phr)	HDDA (phr)
A0	800	0	0
AH1	800	0.03	1.0
AH2	800	0.03	1.5
AH3	800	0.03	2.0
AH4	800	0.03	2.5

The pellets were then injection molded with an injection machine (SZ-550NB, Ningbo Plastic Machine Co., China) with a screw temperature profile of 180–225 °C. The injection molded samples were dumbbell-shaped samples for tensile tests and rectangular samples for impact tests. For rheological measurements, the blended pellets were compression molded at 170 °C and 5 MPa for 3 min to obtain disk-shaped samples with a thickness of 2.0 mm and a diameter of 25 mm.

Gel Determination

The original and modified PPR samples obtained from extruder were packed with filter paper, and then were extracted in the Soxhlet extraction apparatus with xylene for 24 h at 140 °C. No gel was observed for all samples.

Melt Index Measurement

Melt flow indices (MFI) were measured following ISO 1133-97 using a MFI tester (XNR-400, Chengde Desheng Testing Equipments Co., Ltd, China) at 230 °C /2.16kg.

Fourier Transform Infrared Spectroscope (FTIR)

FTIR spectra of all samples were measured at room temperature using a Nicolet 5700 Fourier transform infrared spectroscope (FTIR). The modified PPs were dissolved in hot xylene at 140 °C, and then the solutions were charged into acetone at room temperature. Unreacted HDDA monomer and copolymerized HDDA remained soluble, while PP and PP-*g*-HDDA precipitated out. PP and PP-*g*-HDDA were separated by filtration, and then were dried at 80 °C under vacuum for 48 h. The purified samples were pressed into films for FTIR analysis.

Oscillatory Shear Rheology

The small-amplitude oscillatory shear rheology measurements were carried out with a Bohlin Gemini 200 rheometer (England) equipped with a parallel-plate fixture (25 mm diameter). The gap between the two parallel plates was maintained at 1.75 mm for all these rheological measurements. The measurements were performed as a function of angular frequency (ω) ranging from 0.03 rad/s to 100 rad/s at 190 °C. A fixed maximum strain of 1% was used to ensure that the measurements were carried out within the linear viscoelastic range of the materials.

Mechanical Characterization

Tensile tests were carried out following ISO 527-2:1997 obtain the load-displacement curves and measure the yield strength and stress and strain at break. Dumbbell-shaped specimens of dimensions 115 mm × 10 mm × 4 mm in the narrow section were tested using an electromechanical testing machine (CMT6104, Shenzhen Skyan Power Equipment Co., Ltd, China) at a crosshead speed of 50 mm/min.

Charpy impact tests were performed following ISO 179-1:2000 to determine the impact strength. Injection-

molded rectangular samples with dimensions of 80 mm × 10 mm × 4 mm and a single-edge 45° notch were tested using the Charpy impact tester (XJJ-50, Chengde Jiande Testing Equipments Co., Ltd, China).

DSC Measurements

DSC scanning of the samples was performed on a DSC 200 PC instrument (NETZSCH Group, Germany) in nitrogen atmosphere. Samples of about 5 mg were heated from room temperature to 220 °C at a rate of 20 K/min, and held for 5 min to eliminate thermal history. Then, the samples were cooled to room temperature at 10 K/min, following a second heating from room temperature to 220 °C at a rate of 20 K/min. The first cooling and second heating scans were recorded. The crystallinity is determined by

$$X_c = \Delta H / \Delta H^0 \times 100\% \quad (1)$$

in which ΔH and ΔH^0 are the melting enthalpy of the samples and 100% pure crystalline PP, respectively, with ΔH^0 = 209 J/g[28].

Polarized Light Microscope (PLM) Observations

To investigate the crystalline morphology, a specimen was cut from the injected sample and hot-compressed into a thin film at 240 °C on the hot stage, and held for 5 min to eliminate thermal history. It was then quickly cooled to 160 °C and maintained for 20 min. The crystal morphology was observed by a PLM instrument (XP-213, Nanjing Jiangnan Novel Optics Co., Ltd., China)

Dynamic Mechanical Analysis (DMA)

DMA testing was carried out using a DMA Q800 analyzer (TA Instrument, USA). The single cantilever mode was used, and the measurement was carried out on a rectangular shaped part with the size of 35 mm × 10.2 mm × 4.2 mm (length × wide × thickness) from −60 °C to 110 °C at a heating rate of 3 K/min and an oscillatory frequency of 1 Hz.

RESULTS AND DISCUSSION

Melt Flow Properties

Table 2 lists the MFI results of the virgin and modified PPRs. It is well known that the addition of a polyfunctional monomer can stabilize tertiary macroradicals against scission by assisting in the formation of secondary macroradicals which subsequently lead to the branching reaction. The MFI increased from 2.3 of A0 to 3.98 of AH1, indicating that the degradation reaction is dominant in the presence of a relatively high content of DCP and low content of HDDA, thus resulting in the decrease of its molecular weight. Compared to AH1, the MFI decreased gradually with the increase of HDDA content, which might be due to an increasing degree of LCB in PPR backbone as the result of a high consumption of primary peroxide radicals with the increase of HDDA concentration[19, 20].

Table 2. MFI of virgin and modified PPRs

Sample	A0	AH1	AH2	AH3	AH4
MFI (g/10min)	2.3	3.98	3.37	2.65	1.9

FTIR Spectroscopy

Figure 2 shows the FTIR spectra of the purified samples. For all the samples modified with HDDA, there was a band at about 1733 cm^{-1}, which was ascribed to the stretching vibration of carbonyl group of ester in HDDA molecule. Moreover, the band area at 1733 cm^{-1} seems to increase with increasing HDDA concentration, indicating that more HDDA was grafted onto PPR backbone. From the FTIR spectra, the carbonyl index (CI) was defined as A_{1733}/A_{1163}, where A_{1733} is the band area at 1733 cm^{-1}, characteristic of carbonyl groups of the ester; A_{1163} is the band area at 1163 cm^{-1}, characteristic of the CH_3 groups (stretching of the CH_3 groups on PPR chains). The values of CI are listed in Table 3. CI increases gradually with the increase of HDDA concentration. As reported, CI can be considered as a measure of the content of grafted HDDA (either in a single unit or polychains) on the PPR backbone[29, 30], therefore the changes of CI indicate an increasing grafting degree with

the increase of HDDA concentration. However, CI is unable to differentiate the structure of long- versus short-branched chains. The linear viscoelastic behavior was very sensitive to the LCB of the polymer.

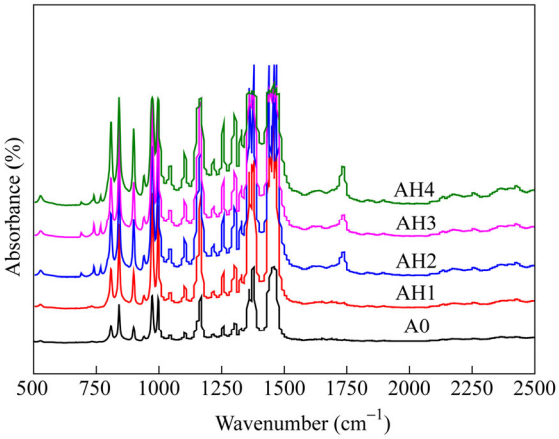

Fig. 2 FTIR spectra of the purified samples

Table 3. CI of purified PPR samples

Sample	A0	AH1	AH2	AH3	AH4
CI	0	0.17	0.26	0.31	0.36

Linear Viscosity Properties

Oscillatory shear rheology is useful for the detection of LCB, being very sensitive to LCB structure, and can be used to demonstrate the existence of even a very low level of LCB directly[7, 31, 32]. The presence of a very low amount of LCB can change the zero shear viscosity (η_0) and shear thinning degree[33]. Figure 3 shows the complex viscosity (η^*) versus sweeping frequency (ω) curves of the virgin and modified PPRs. In the presence of DCP, when a very low amount of HDDA was used (AH1), the complex viscosity decreased obviously at low frequency and the Newtonian-zone became broader, implying that the degradation reaction induced by DCP was dominant in sample AH1, although there might be a small fraction of grafted molecules in the presence of the HDDA[21]. When the amount of HDDA was increased, complex viscosity curves became higher and the shear thinning behavior was strengthened, indicating that the addition of more HDDA reduced the degradation reaction. Besides, the complex viscosities of modified PPR with a relatively high amount of HDDA (AH4) were higher than those of A0 at low frequency but lower than those of A0 at high frequency. Considering the fact that no gel was observed, indicating that no crosslinking was formed in all the modified samples, the rheological behavior could be interpreted as the typical character of polymers with long chain branching[34].

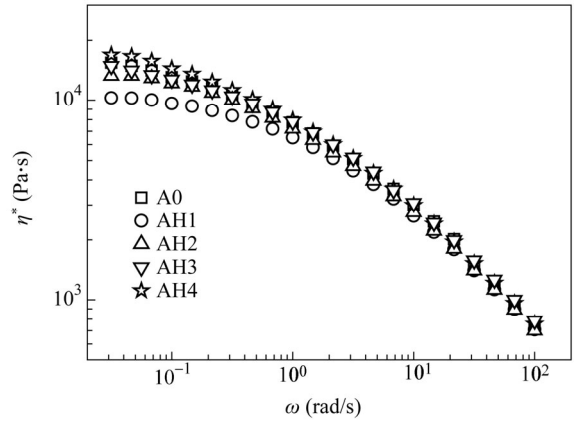

Fig. 3 Complex viscosity versus sweeping frequency for virgin and modified PPRs at 190 °C

In order to quantify the rheological behavior, the viscosity versus frequency curves of the samples were fitted by the following equation[35]

$$\eta^*(\omega) = \frac{\eta_0}{1+(\lambda\omega)^{\alpha}} \tag{2}$$

where η_0 is the zero-shear viscosity, λ is a relaxation time which inversely accounts for the onset of the shear-thinning region, and α is a shear-thinning index. These values for virgin and modified PPRs are listed in Table 4. Furthermore, the viscosity data at high frequency were fitted by Eq. (3):

$$\eta^* = m\omega^{n-1} \tag{3}$$

where m is the consistency and n is the power-law exponent, which indicates the degree of non-Newtonian behavior. The smaller the value of n, the more pronounced the shear-thinning phenomenon. The values of n for all the samples are also included in Table 4. Compared to AH0, AH1 showed decreased values of η_0 and λ, and increased values of α and n, indicating that both the degradation and grafting reaction existed in the presence of DCP and HDDA, while the degradation was dominant when a low amount of HDDA was included. For the modified PPRs, the values of η_0 and λ increase, while the values of α and n decreased gradually with increasing amount of HDDA, which suggests that the increasing LCB content led to a longer relaxation time and a more pronounced shear-thinning phenomenon.

Table 4. Rheological parameters of origin and modified PPRs

Sample	$\eta_0 \times 10^{-4}$ (Pa·s)	λ (s)	α	n	Terminal slope of G'
A0	1.82	1.73	0.57	0.75	1.15
AH1	1.12	0.59	0.65	0.78	1.52
AH2	1.50	1.07	0.64	0.75	1.27
AH3	1.68	1.31	0.59	0.73	1.12
AH4	2.11	2.44	0.57	0.71	1.03

Besides the complex viscosity, the storage modulus (G') is also very sensitive to the presence of LCB. The curves of G' as a function of ω for the virgin and modified PPRs are shown in Fig. 4. It was observed that A0 and AH1 exhibited the typical terminal behavior. For A0, this is due to its linear molecular chain structure, while for AH1, the DCP induced degradation reaction played a dominant role. As a result, most of the macromolecular chains of AH1 were linear and yielded a lower molecular weight compared to A0, thus a lower value of G' at low frequency was seen in AH1. With the increase of HDDA concentration, the values of G' for modified PPRs increased at low frequency and the terminal slope decreased gradually, the values of which are

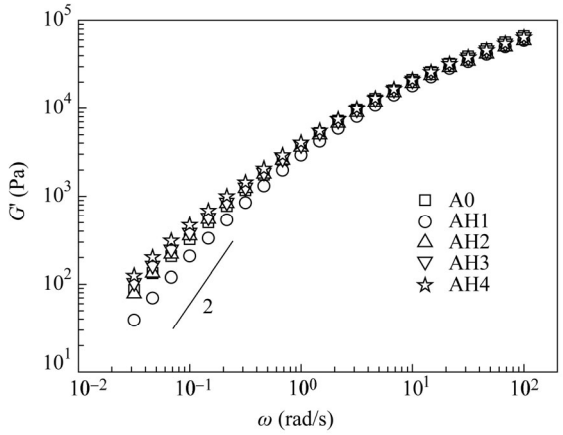

Fig. 4 The curves of storage modulus versus sweeping frequency for the virgin and grafted PPRs at 190 °C (The line with a slope of 2 is inserted for comparison.)

listed in Table 4. In general, the terminal slope, which was 1.15 for A0, decreased from 1.52 of AH1 to 1.03 of AH4. Similar results were reported by Tian *et al*[7]. The non-terminal behavior was related to the existence of LCB in their skeleton leading to the longer relaxation mechanism, indicating the formation of long chain branches from radical reactions.

It has been reported that the loss angle (δ) or tanδ of polyethylene with LCB is independent of frequency in a limited range since they have a gel-like rheological behavior[36]. However, for LCB PPs, it was found that they only showed an inflection in the curve of loss angle and no evident plateau had been found. Similar results of tanδ versus ω for virgin and modified PPRs are found in our system, as shown in Fig. 5. The curve for A0 descended rapidly with increasing frequency, which is a terminal behavior of liquid-like materials. When a low content of HDDA was added in the reaction system, tanδ became higher at low frequency due to the dominant degradation reaction induced by DCP. However, with the increase of HDDA amount, the modified samples exhibited lower values of slope at low frequency and the "plateau" of the loss angle became more evident, indicating that a large number of LCBs were present in the backbone of PPR, which agreed well with the above results. This maybe owed to the gradually reduced ratio of degradation to branching reaction; both could occur simultaneously in the presence of DCP and HDDA.

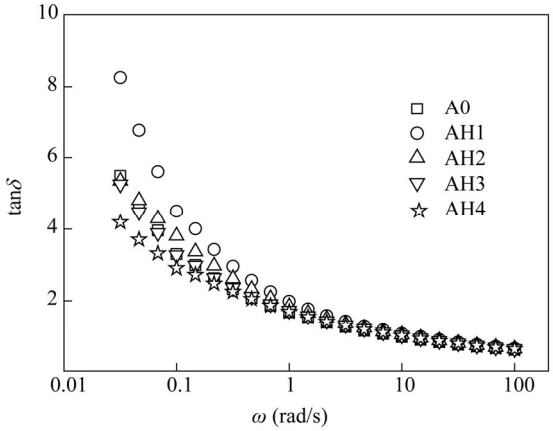

Fig. 5 The curves of tanδ versus sweeping frequency for the virgin and grafted PPRs at 190 °C

The relaxation process can be estimated by a Cole-Cole plot (η''-η'). Figure 6 displays the Cole-Cole plots of virgin and modified PPRs. As expected, A0 exhibited almost a semicircular pattern because of its linear chain structure. With the introduction of a very low amount of HDDA, AH1 also showed semicircular pattern with a decreased radius of the semicircle because of the dominant degradation reaction, although the grafting reaction also existed. With the concentration of HDDA further increasing, the Cole-Cole plots of the modified PPRs were higher than those of the initial PP and showed more evident upturning at high viscosity, indicating that these samples had longer relaxation time.

Effect of LCB on Melting and Crystallization Behavior

The branching reaction between linear PPR, DCP, and HDDA would result in change of the molecular weight, molecular weight distribution, and the chain irregularity. All these microstructure changes could affect the thermal properties of PPR. The DSC heating thermograms of virgin and modified PPRs are shown in Fig. 7(a). The melting temperature (T_m), enthalpies of fusion (ΔH_m) and crystallinity (X_c) of the virgin and modified PPRs are listed in Table 5. It can be seen that the thermograms for virgin and modified PPRs all show a single melting peak. T_m of modified PPRs were almost constant with the addition of DCP and HDDA; however, the shape of melting peaks for the modified PPRs were broader than that of virgin PPR, which is similar with the results reported by Tian *et al.*[37], suggesting that the crystallites of the virgin PPR were more perfect than those of the modified PPRs. However, the shoulder in the melting curves reported by Tian *et al*. was not obvious in our modified PPRs, which might be due to the different testing conditions and different sensitivity of the DSC tester.

As shown in Table 5, the X_c of the modified PPRs was slightly higher than that of virgin PPR, which maybe because the HDDA induced LCBs could act as nucleating agents and help to increase the crystallinity of PPR. The increase of crystallinity with increasing HDDA concentration could also contribute to the increase of yield strength, which was mentioned above.

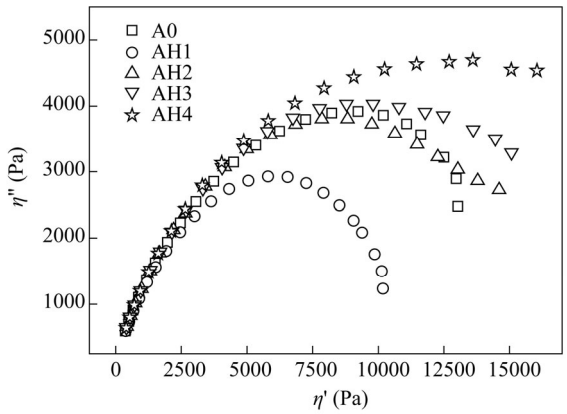

Fig. 6 Cole-Cole plots of virgin and modified PPRs at 190 °C

Figure 7(b) shows the first cooling thermograms of the virgin and modified PPRs. Compared to virgin PPR, all of the modified PPRs showed an increased crystallization temperature (T_c), and T_c increased gradually with increasing amount of HDDA. T_c of AH4 increases by 8.7 K compared to that of A0. Curves of relative crystallinity versus crystallization time for linear and modified PPRs are shown in Fig. 8. The corresponding values of $t_{1/2}$ are included in Table 5, which suggests a gradually increased crystallization rate with the increase of HDDA concentration.

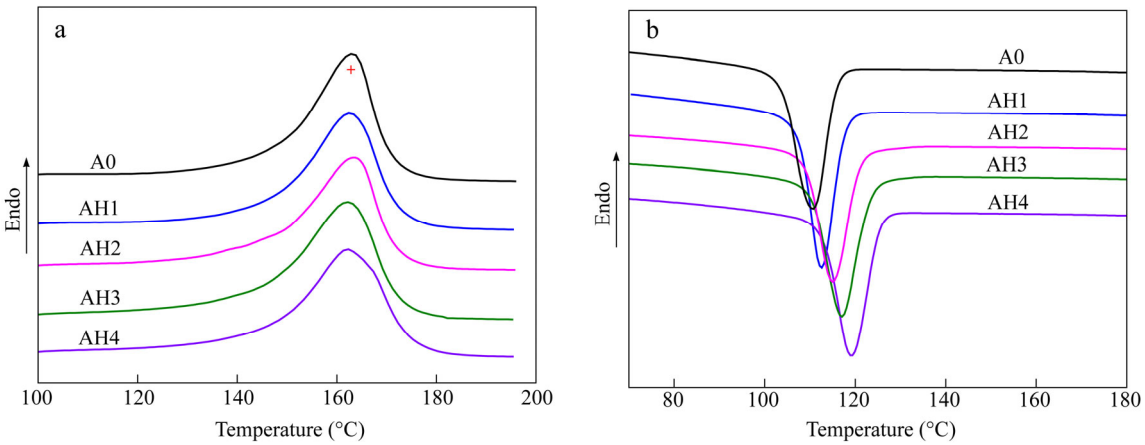

Fig. 7 DSC heating (a) and cooling curves (b) of virgin and modified PPRs

Table 5. Melting and crystallization parameters of virgin and modified PPRs

	T_m (°C)	T_c (°C)	X_c (%)	$t_{1/2}$ (s)	n	Z_c
A0	162.8	110.7	38.7	549	2.67	0.547
AH1	162.4	112.6	39.6	532	1.92	0.664
AH2	163.2	114.9	39.8	523	2.38	0.557
AH3	162.2	117.1	40.2	506	2.42	0.560
AH4	162.3	119.4	41.3	498	1.75	0.675

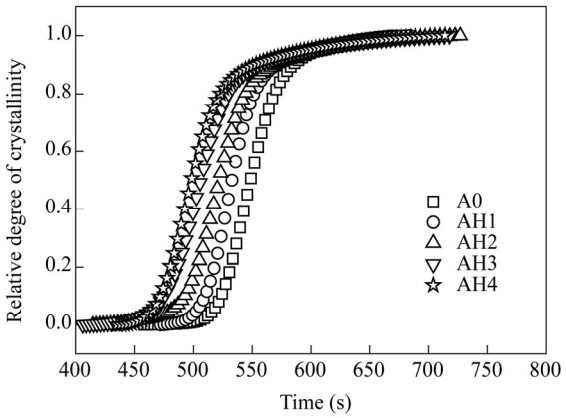

Fig. 8 Evolution of relative crystallinity as a function of crystallization time for PPR and modified PPRs during cooling at 10 K/min

On the basis of the assumption that the crystallization temperature is constant, the Avrami equation can be directly used to describe the primary stage of nonisothermal crystallization. In this case, the Avrami equation is expressed as

$$1 - X(t) = \exp(-Z_t t^n) \tag{4}$$

where Z_t is the rate constant in the nonisothermal crystallization process, n is a mechanism constant depending on the type of nucleation, and growth process parameters. The double-logarithmic form of Eq. (4) is

$$\lg[-\ln(1 - X(t))] = \lg Z_t + n \lg t \tag{5}$$

Considering the nonisothermal character of the process investigated, the final form of the parameter characterizing the kinetics of nonisothermal crystallization was given by Eq. (6).

$$\lg Z_c = \lg Z_t / \varphi \tag{6}$$

where Z_c is the modified crystallization rate constant considering cooling rate φ. Plots of $\lg[-\ln(1-X(t))]$ versus $\lg t$ for virgin and modified PPRs are displayed in Fig. 9. Each curve shows only the linear portion, and the nonlinear part deviated from Avrami equation at high relative crystallinity region is not included. Z_t and n were obtained from the intercept and slope, respectively, while Z_c was estimated according to Eq. (6). The values of n and Z_c were listed in Table 5. The value of n was 2.67 for A0, while it decreased and varied from 1.75 to 2.38 for the modified PPRs, indicating that the introduction of LCB influenced the mechanism of nucleation and the crystal growth geometry of PPR. The value of Z_c for AH1 to AH4 was higher than that of virgin PPR, and

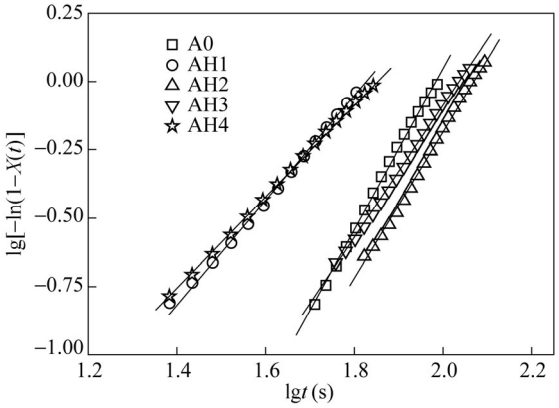

Fig. 9 Plots of $\lg[-\ln(1-X(t))]$ versus $\lg t$ for virgin and modified PPRs

increased with the HDDA concentration increasing, suggesting a higher crystallization rate for the modified PPRs. It is well known that the degradation of macromolecules can result in the improved mobility of the molecular chains and favor the diffusion and arrangement of the macromolecules into crystals. Furthermore, it could be inferred that the branching structure in the backbone of modified PPRs was beneficial for the enhancement of T_c and was also responsible for the acceleration in crystallization. One possible explanation is that HDDA induced LCBs act as nucleating agents and a large number of nuclei is formed in the initial stage of crystallization.

Effect of LCB on Crystalline Morphology

To further investigate the crystallization properties of the samples, the spherulitic morphology of the virgin and modified PPRs was observed by PLM, and the results are shown in Fig. 10. The spherulites of the virgin PPR were well developed, resulting in a ‘‘Maltesecross’’ structure with large spherulite size and a broad distribution of the spherulite dimensions. With the addition of DCP and HDDA (AH1), more nucleation sites and smaller spherulites are shown, although one can still observe a small number of spherulites with relatively large size. With the increase of HDDA level, many more nucleation sites and much smaller spherulites could be observed. The size of the spherulites became more even, the number of the spherulites increases and the dimensions of spherulites decreased with the increase of HDDA concentration. These changes are due to the LCB acting as nucleating agents and inducing larger numbers of spherulites[38, 39]. Since more spherulites grow in a confined space, they tend to squeeze together, resulting in smaller size. The results of PLM are in accordance with the above DSC results, and both indicate the nucleation effect of LCB in modified PPRs, which gives rise to numerous nuclei in the initial stage of crystallization.

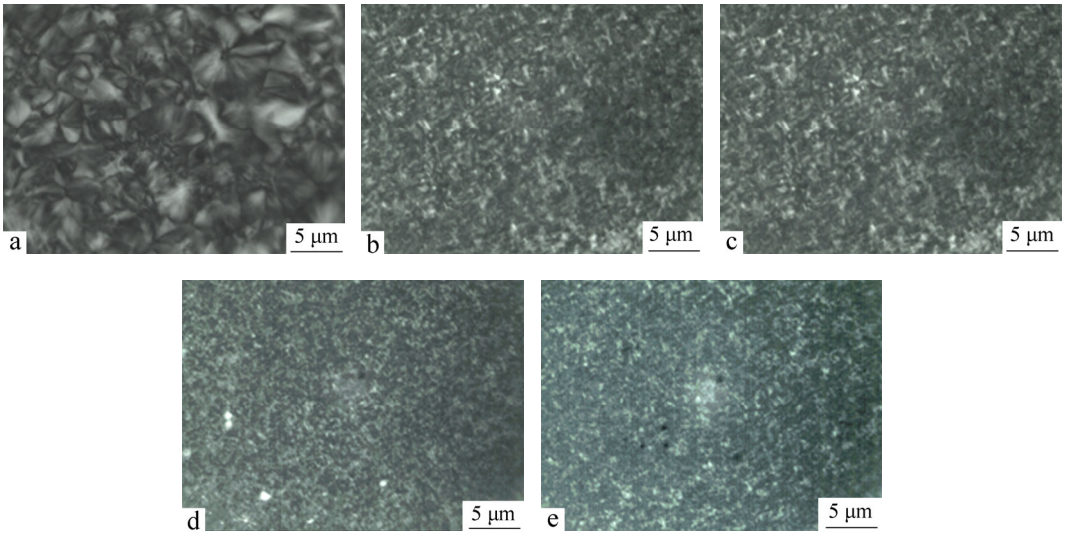

Fig. 10 PLM photographs of crystal morphologies for PPR (a), AH1 (b), AH2 (c), AH3 (d) and AH4 (e)

Mechanical Properties

In order to study the effect of LCB on the mechanical properties of PPT, Charpy impact tests and tensile tests were applied to all of the samples. Figure 11 shows the Charpy impact strength of the virgin and modified PPRs. As is shown, the value of the impact strength of AH1 was nearly twice that of A0. With the increase of HDDA content, the impact strength increases gradually further, reaching a maximum value of 3.6 kJ/m^2, compared to 1.7 kJ/m^2 for that of the virgin PPR. The improvement of impact strength could be explained mainly by the spherulite size, which were much smaller for the modified PPRs than for A0. The smaller and finely dispersed crystal structures, uniform distribution of the spherulites and the higher crystallinity of the modified PPRs, as demonstrated above, contribute to the elevated impact strength of the modified PPRs. Another important factor

affecting the impact strength is the molecular structure. The LCB induced molecular chain entanglements could increase the molecular interactions[40] and act as physical cross-link points, which absorbed more energy during impact fracture, while the possible breakage of molecular chains induced by DCP resulted in improved mobility of the molecular chains and favored the movement of the chain segments, which also consumed higher energy during impact failure.

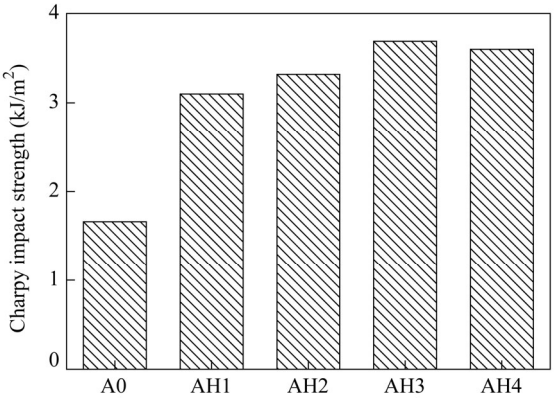

Fig. 11 Charpy impact strength of virgin and modified PPRs

Typical load-displacement curves for virgin and modified PPRs are shown in Fig. 12, and the calculated results of tensile properties, as illustrated by yield strength and elongation at break are shown in Fig. 13. The yielding peaks of the modified PPRs were broader than that of virgin PPR, as shown in Fig. 12; in other words, the modified PPRs exhibited a slower necking rate than the virgin PPR. Also, it is shown that the modified PPRs other than for AH1 showed higher yield strength compared to virgin PPR in Fig. 13(a). It is known that yielding in polymers is related to the onset of orientation of the molecular chains, slippage between molecules and the rearrangement of the microcrystals, while the fracture is mainly because of the breakage of molecules and slippage between molecules. For the modified PPRs, especially those with high LCB levels, it was not only the chemical bonds and van der Waals forces, but also the entanglements of molecules that resisted the tensile stress. Thus the changes in tensile properties could be explained mainly by LCB induced molecular chain entanglement in the modified PPRs, leading to a lower speed of molecular orientation and higher yield strength. In addition, the increased crystallinity and the larger number of microcrystallites in the modified PPRs, especially for those with high HDDA concentrations, were also responsible for the changes in yielding.

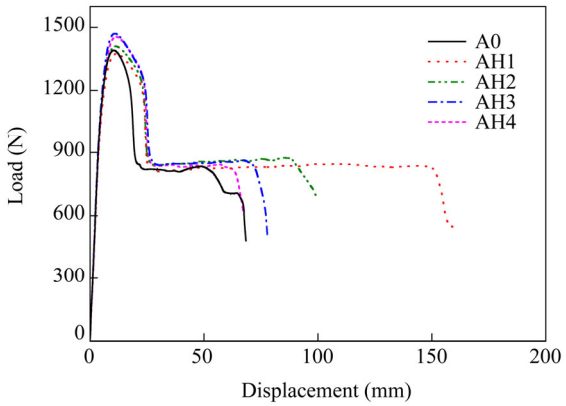

Fig. 12 Typical load-displacement curves for various samples

The value of the elongation at break of PPR was about 2.5 times as much as that of A0, as shown in Fig. 13(b), which was attributed to the dominant contribution of DCP at a low HDDA concentration. A similar

phenomenon was reported by Salazar *et al*[28]. The authors attribute the improvement in strain at break to the entanglement density which diminishes in the presence of DCP, and such decrease in entanglements favor the slippage of molecular chains during elongation, giving rise to higher breaking strain[28]. The elongation at break decreased obviously when more HDDA was introduced, and seemed not to be influenced by the amount included at high HDDA concentration levels. As is known, the toughness of polymer samples can be illustrated by both the impact strength and tensile elongation at break. However, in our experiment, a different variation trend was found in elongation at break from that in the impact strength. Considering the fact that no gel has been found in all samples, it may be because the LCBs induced chain entanglement restricts the extension of molecular chains during tensile tests and thus leads to decreased elongation at break for modified samples.

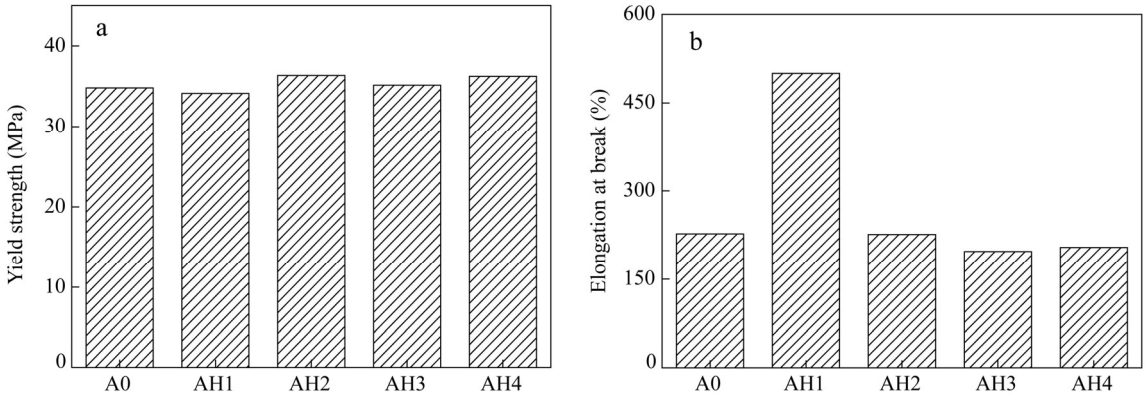

Fig. 13 Yield strength (a) and elongation at break (b) of virgin and modified PPRs

Effect of LCB on Molecular Mobility

To further understand the effect of LCB on the crystallization and mechanical properties, the molecular motions in amorphous region were investigated by using DMA. The dependence of storage modulus (G'), loss modulus (G'') and loss tangent (tanδ) on temperature for the virgin PPR and two of the modified PPRs, namely AH2 and AH4, is displayed in Fig. 14. The curves of both G' and G'' showed an obvious increase for the modified PPRs compared to virgin PPR, especially in the low temperature range. The increase of G' indicates the improvement of modulus and strength at low temperatures, which agrees well with the change in tensile strength, while the increase of G'' suggests that the modified samples contains more soft molecular chains in the amorphous phase than virgin PPR, which contributes less to energy dissipation during fracture. Further evidence for the increase of molecular mobility comes from the shift of the G'' peak to lower temperature with the addition of HDDA.

The mechanical loss tangent is thought to be more useful than G' and G'' to exhibit the microstructure change. The maximum at low temperature (about 18 °C) is related to the β relaxation, corresponding to the glass transition (T_g) of the unrestricted amorphous PP, while the peak at the higher temperature (about 85 °C) is related to the α relaxation, corresponding to the relaxation of restricted PP amorphous chains in the crystalline phase (defects), also known as the rigid amorphous molecules[41]. As shown in Fig. 14(c), T_g of the modified PPRs decreased by 4 K compared to virgin PPR, implying a slightly improved mobility of the molecular chain segments. Wang *et al*.[34] has shown that the long chain branching was the determining factor in controlling the rheological properties of polymer melts while the short chain branching played a decisive role in affecting the dynamic mechanical properties. Thus the change of T_g and molecular mobility could possibly be explained by the simultaneous existence of a small fraction of short chain branching (SCB) and of the LCB, and the SCB would be due to the coexistence of degradation and branching reactions in the presence of DCP and HDDA, which would possibly give rise to a certain concentration of relatively short molecule chains or branches. This would increase the amount of mobile amorphous phase available in the PPR, although there would be a dominant fraction of LCB, as demonstrated above. This improved mobility of molecular chain segments was

beneficial to the crystallization and toughness. Therefore, the characteristics of molecular structure, the crystallization properties as well as the crystalline morphology can account for the changes of the mechanical properties.

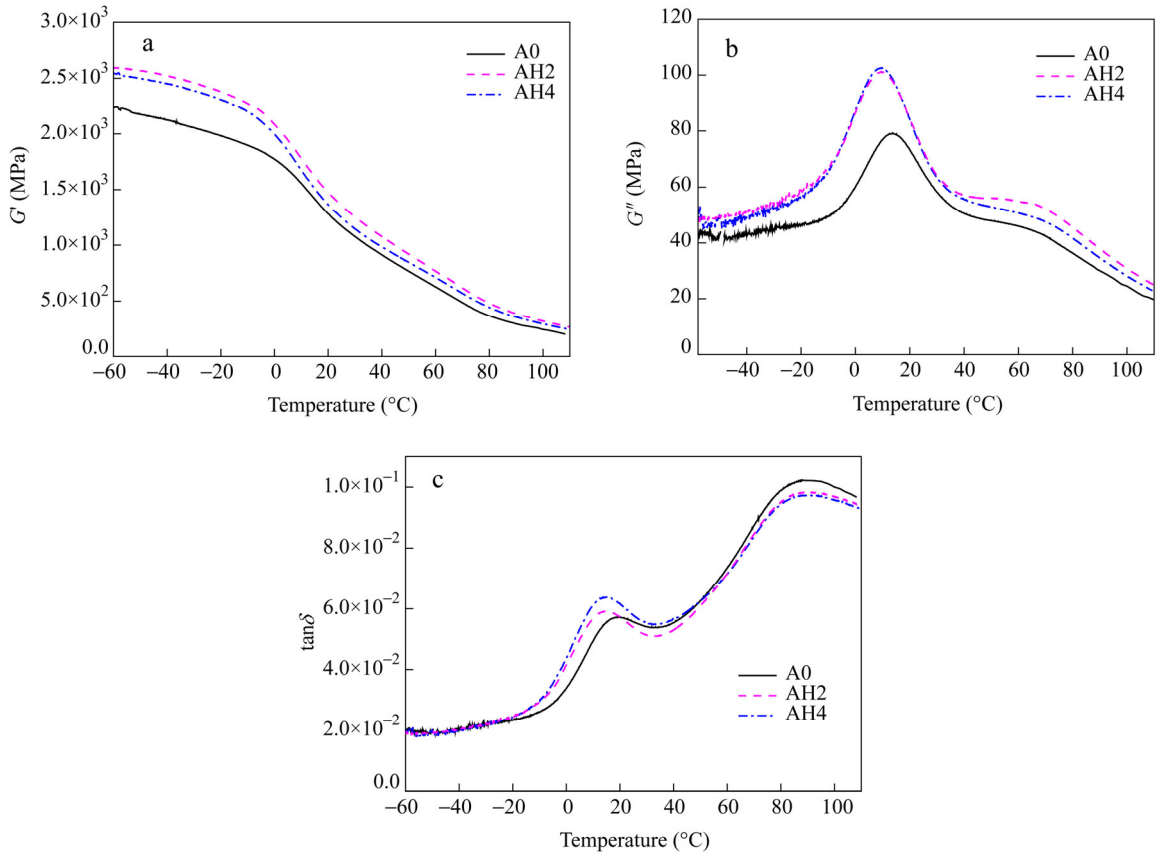

Fig. 14 Dependence of storage modulus (G') (a), loss modulus (G'') (b) and loss tangent (tanδ) (c) on temperature for A0, AH2 and AH4

CONCLUSIONS

LCB-PPRs were prepared by the addition of 0.03 phr DCP and various amounts of HDDA into linear PPR *via* reactive extrusion. It was found that the MFI increased first and then decreased gradually with the addition of HDDA amount. FTIR results demonstrated the grafting reaction occurred in the modified PPRs; and the grafting degree increased with increasing HDDA concentration. The rheological complex viscosity, G' and tanδ versus ω plots, as well as the Cole-Cole plots confirmed that the LCB structure was introduced into the modified PPRs skeleton after modification. The results of DSC and PLM both demonstrated that DCP and HDDA induced the LCBs to act as nucleating agents and accelerated the crystallization process significantly. In addition, the nucleating effect became more obvious with the increase of HDDA concentration. In the amorphous phase, more soft molecular chains and an improved mobility of molecular chain segments were found. The changes in both crystalline and amorphous phases, as well as the LCB induced molecular chain entanglements contribute to the changes in mechanical properties. Compared to virgin PPR, the modified PPRs exhibited significantly higher impact strength, which showed an increasing trend with the increase of HDDA concentration. The results of the tensile tests showed a relatively constant value of yield strength and an increased value of elongation at break for a very low amount of HDDA, and then a slight increase of yield strength and an obvious decrease of elongation at break when the amount of HDDA was further increased.

REFERENCES

1 Ficker, H.K. and Walker, D.A., Plast. Rubber. Process. Appl., 1990, 14: 103
2 Karger-Kocsis, J., "Polypropylene: Structure, blends and composites", Chapman and Hall: London, 1995, Volume 2
3 Mileve, D., Androsch, R. and Radusch, H.J., Polym. Bull., 2008, 61: 643
4 Wang, Y., Cheng, S. and Wang, S.Q., J. Rheol., 1998, 14: E5
5 Lagendijk, R.P., Hogt A.H., Buijtenhuijs, A. and Gotsis, A.D., Polymer, 2001, 42: 10035
6 Tang, H.X., Dai, W.L. and Chen, B.Q., Polym. Eng. Sci., 2008, 48: 1339
7 Tian, J.H., Yu, W. and Zhou, C.X., Polymer, 2006, 47: 7962
8 Auhl, D., Stange, J. and Münstedt, H., Macromolecules, 2004, 37: 9465
9 Zhang, Z.N., Yu, F.Y., Yu, W. and Zhang, H.B., J. Polym. Res., 2015, 22: 198
10 He, C.X., Costeux, S., Wood-Adams, P. and Dealy, J.M., Polymer, 2003, 44: 7181
11 Gotiss, A.D., Zeevenhoven, B.L.F. and Hogt, A.H., Polym. Eng. Sci., 2004, 44: 973
12 Weng, W., Hu, W., Dekmerzian, A.H. and Ruff, C.J., Macormolecules, 2002, 35: 3838
13 Langston, J.A., Colby, R.H., Chung, T.C.M., Shimizu, F., Suzuki, T. and Aoki, M., Macromolecules, 2007, 40: 2712
14 Langston, J.A., Colby, R.H., Shimizu, F. and Suzuki, T., Macromol. Symp., 2007, 260: 34
15 Krause, B., Stephan, M. and Volkland, S., J. Appl. Polym. Sci., 2005, 99: 260
16 Ali, Z.I., Youssef, H.A., Said, H.M. and Saleh, H.H., Adv. Polym. Technol., 2006, 25: 208
17 Borsig, E., Duin, M.V., Gotsis, A.D. and Picchioni, F., Eur. Polym. J., 2008, 44: 200
18 Graebling, D., Macromolecules, 2002, 35: 4602
19 Su, F.H. and Huang, H.X., J. Appl. Polym. Sci., 2009, 113: 2126
20 Su, F.H. and Huang, H.X., Adv. Polym. Technol., 2009, 28: 16
21 Yamaguchi, M. and Wagner, M.H., Polymer, 2006, 47: 3629
22 Hadjichristidis, N., Xenidou, M., Iatrou, H., Pitsikalis, M., Poulos, Y., Avgeropoulos, A., Sioula, S., Paraskeva, S., Velis, G., Mendelson, R.A., Garcia-Franco, C.A., Sun, T. and Ruff, C.J., Macromolecules, 2000, 33: 2424
23 Cotts, P.M., Cuan, Z., McCord, E. and McLain, S., Macromolecules, 2000, 33: 6945
24 Wang, W.J., Kharchenko, S., Migler, K. and Zhu, S., Polymer, 2004, 45: 6495
25 Xing, H., Jiang, Z., Zhang, Z., Qiu, J., Wang, Y., Ma, L. and Tang, T., Polymer, 2012, 53: 947
26 DeGrott, A.W., Karjala, T.P., Taha, N. and Johnson, M.S., "Long chain branching measurements of polyethylenes: a tool-box of techniques. Paper presented at international workshop on branched polymers for performance", Spring 2004
27 McKee, M.G., Unal, S. and Long, T.E., Prog. Polym. Sci., 2005, 30: 507
28 Salazar, A., Rodríguez, S., Navarro, J.M., Ureña, A. and Rodríguez, J., E-polymers, 2007, no. 021
29 Wan, D., Li, M., Zhang, Z., Xing H., Wang, L., Jiang, Z., Zhang, G. and Tang, T., Polym. Degrad. Stab., 2012, 97: 40
30 Su, F.H. and Huang, H.X., Polym. Eng. Sci., 2010, 50: 342
31 Wang, L., Wan, D., Zhang, Z.J., Liu, F., Xing, H.P., Wang, Y.H. and Tang, T., Macromolecules, 2011, 44: 4167
32 Zhao, W.Y., Huang, Y.J., Liao, X. and Yang, Q., Polymer, 2013, 54: 1455
33 Malmberg, A., Gabriel, C., Steffl, T., Mu¨nstedt, H. and Lo¨fgren, B., Macromolecules, 2002, 35: 1038
34 Wood-Adams, P.M. and Dealy, J.M., Macromolecules, 2000, 33: 7489
35 Cross, M.M.J., Colloid. Sci., 1965, 20: 417
36 Franco, C.G., Srinivas, S. and Lohse, D.J., Macromolecules, 2001, 34: 3115
37 Tian, J.H., Yu, W. and Zhou, C.H., J. Appl. Polym. Sci., 2007, 104: 3592
38 Gohil, R.M. and Phillips, P.J., Polymer, 1986, 27: 1687
39 Ferrer-Balas, D., Maspoch, M.L., Martinez, B. and Santana, O.O., Polymer, 2001, 42: 1697
40 Nielsen, L.E and Landel, R.F., "Mechanical properties of polymers and composites", 2nd ed., Marcel Deker, New York, 1994
41 Read, B.E., Polymer, 1989, 30: 1439